ERAD deficiency promotes mitochondrial dysfunction and transcriptional rewiring in human hepatic cells

Received for publication, April 21, 2020, and in revised form, September 15, 2020 Published, Papers in Press, September 25, 2020, DOI 10.1074/jbc.RA120.013987

Qingqing Liu[1,‡], Xiaoqin Yang[1,‡], Guangyu Long[1], Yabing Hu[1], Zhenglong Gu[2], Yves R. Boisclair[3], and Qiaoming Long[1,*]

From the [1]Jiangsu Key Laboratory of Neuropsychiatric Diseases and Cam-Su Mouse Genomic Resources Center, Medical College of Soochow University, Suzhou, Jiangsu Province, China, the [2]Division of Nutritional Sciences, Cornell University, Ithaca, New York, USA and the [3]Department of Animal Science, Cornell University, College of Agriculture and Life Sciences, Ithaca, New York, USA

Edited by Peter Cresswell

Mitochondrial dysfunction is associated with a variety of human diseases including neurodegeneration, diabetes, nonalcohol fatty liver disease (NAFLD), and cancer, but its underlying causes are incompletely understood. Using the human hepatic cell line HepG2 as a model, we show here that endoplasmic reticulum-associated degradation (ERAD), an ER protein quality control process, is critically required for mitochondrial function in mammalian cells. Pharmacological inhibition or genetic ablation of key proteins involved in ERAD increased cell death under both basal conditions and in response to proinflammatory cytokines, a situation frequently found in NAFLD. Decreased viability of ERAD-deficient HepG2 cells was traced to impaired mitochondrial functions including reduced ATP production, enhanced reactive oxygen species (ROS) accumulation, and increased mitochondrial outer membrane permeability. Transcriptome profiling revealed widespread down-regulation of genes underpinning mitochondrial functions, and up-regulation of genes associated with tumor growth and aggression. These results highlight a critical role for ERAD in maintaining mitochondrial functional and structural integrity and raise the possibility of improving cellular and organismal mitochondrial function via enhancing cellular ERAD capacity.

The endoplasmic reticulum (ER) serves several critical cellular functions, including Ca^{2+} storage, lipid synthesis, and the folding of protein molecules destined for the secretory pathway. Impaired ER function or ER stress has been implicated in an increasing number of chronic human diseases, including obesity, diabetes, neurodegeneration, nonalcohol fatty liver disease (NAFLD), and cancer (1–3). ER stress is an abnormal homeotic condition characterized by the accumulation of unfolded or misfolded proteins in the ER lumen (4). The classical view is that ER stress activates the unfolded protein response (UPR), which is coordinated by the ER stress sensors, PERK, IRE1a, and ATF6 (5). Activation of these sensors reduces protein translation and enhances protein folding and ER-associated degradation (ERAD). Failure of these actions to restore homeostasis results in sustained ER stress, activation of the CCAAT-enhancer–binding protein homologous protein (CHOP) pathway and apoptosis (6).

The ER is a well-characterized "functional partner" of many organelles and dysregulation of these interactions may impair cellular function (7). The interactions between the ER and mitochondria, an organelle essential for life and death of eukaryotic cells (8–10), provide a good example of the importance of this partnership. The ER and mitochondria form tight physical contacts at the mitochondria-associated membranes (MAMs) to regulate several key cellular processes, including Ca^{2+} homeostasis, lipid exchange, steroid biosynthesis, and apoptosis (11). The MAMs were also found to function as a signaling hub for mitochondria fission as well as autophagy, key events involved in mitochondrial quality control (12). Over the last few years, biochemical and genetic approaches have provided evidence how these two organelles interact physically and functionally to coordinate various cellular functions (13, 14). However, less is known about the potential pathophysiological consequences of an impaired UPR pathway in the ER on mitochondria function and vice versa.

We have recently reported that pharmacological and genetic disruption of ERAD, an ER protein quality control process, impairs glucose-stimulated insulin secretion in cultured rat pancreatic β-cell line and in mice (15). By utilizing an ERAD-deficient hepatic cell line model, we demonstrate here that ERAD deficiency causes structural and functional damages to mitochondria. Consequently, ERAD-deficient cells show impaired ATP production, increased mitochondrial outer membrane permeability (MOMP), and enhanced sensitivity to tumor necrosis factor α (TNFα)-induced cell death. These consequences of ERAD deficiency were associated with an altered gene expression profile characterized by the selective down-regulation of mitochondria-related and up-regulation of tumor growth and aggression-related genes. These results indicate that ERAD is critically required for maintaining normal mitochondrial function and ERAD deficiency may potential mammalian cells to adopt a tumorigenic molecular signature by activating the mitochondrial retrograde signaling pathway.

This article contains supporting information.
‡These authors contributed equally to this work.
* For correspondence: Qiaoming Long, qmlong@suda.edu.cn.

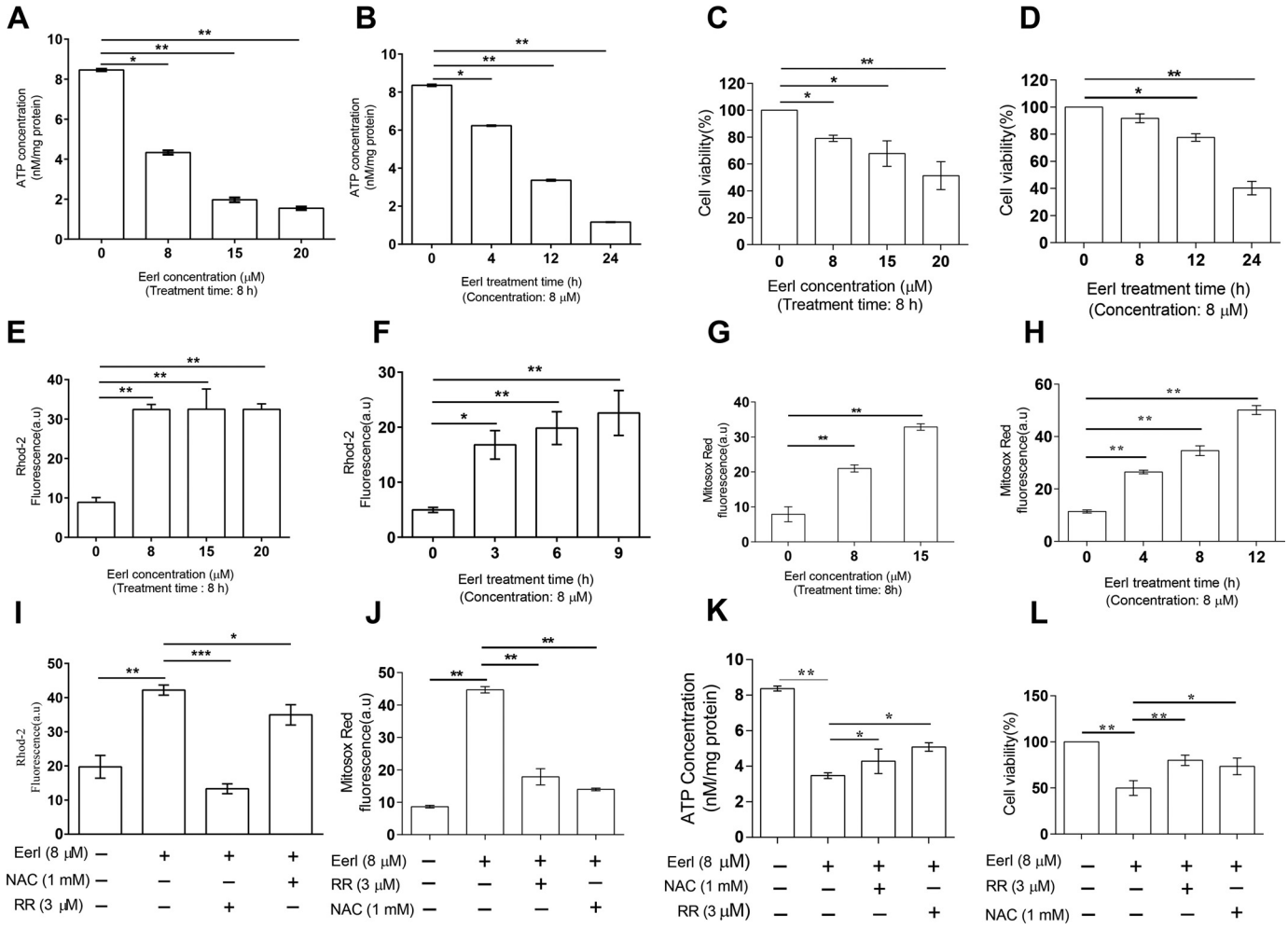

Figure 1. Pharmacological inhibition of ERAD perturbs mitochondrial function and reduces cell viability. HepG2 cells were seeded into 6-well–plates at an initial density of 1×10^5/well and allowed to recover for 12 h before treating with Eerl and other chemical reagents (RR, 2-APB, and NAC). Following the treatments, HepG2 cells were analyzed for: *A* and *B,* cellular ATP concentration; *C* and *D,* cell viability; *E* and *F,* mitochondrial Ca^{2+}; and *G* and *H,* mitochondrial ROS levels. *I–L*, antagonizing effect of RR or NAC on Eerl-induced increase of mitochondrial Ca^{2+} (*I*) and ROS (*J*); and decrease of ATP production (*K*), and cell viability (*L*). All data are mean ± S.E. ($n = 3$). *, $p < 0.05$; **, $p < 0.01$ by Student's *t* test.

Results

Pharmacological inhibition of ERAD perturbs HepG2 cell mitochondrial function and reduces cell viability

We recently showed that ERAD disruption reduces ATP production in rat pancreatic β-cell line INS-1, indicating that ERAD deficiency impairs mitochondrial respiratory function (15). To determine whether this phenomena extends to other mammalian cells, we treated human hepatic HepG2 cells with the ERAD inhibitor eeyarestatin I (EerI). EerI treatment caused dose- and time-dependent decreases in ATP levels (Fig. 1, *A* and *B*) and cell viability (Fig. 1, *C* and *D*). These dose- and time-dependent EerI effects were associated with reciprocal increases in mitochondrial levels of calcium (Ca^{2+}) (Fig. 1, *E* and *F*) and ROS (Fig. 1, *G* and *H*).

Next we tested the roles of increased of mitochondrial Ca^{2+} and ROS in mediating the effects of EerI on ATP levels and cell viability. HepG2 cells were treated with EerI in the absence or presence of the mitochondrial Ca^{2+} uptake inhibitor ruthenium red (RR) and the ROS scavenger *N*-acetylcysteine (NAC). As expected, the stimulatory effects of EerI were reversed by RR in the case of mitochondrial Ca^{2+} and by both RR and NAC in the case of ROS (Fig. 1, *I* and *J*). More importantly, both RR and NAC attenuated the negative effects of EerI on ATP levels and cell viability (Fig. 1, *K* and *L*). These results indicate that an effective ERAD is required to maintain normal mitochondrial function and cell viability in mammalian cells.

Genetic ablation of the ERAD core protein SEL1L sensitizes HepG2 cells to pro-inflammatory cytokine-induced cell death

Mammalian SEL1L is essential for the formation of the ERAD complex on the ER membrane. To further assess the role of ERAD for normal mitochondrial function, we used CRISPR/Cas9-based gene editing to generate 3 independent SEL1L-deficient ($Sel1l^{-/-}$) HepG2 cell lines (Fig. 2, *A* and *B*). Although the SEL1L-deficient cell lines were viable and morphologically undistinguishable from the parental HepG2 cell line, they showed markedly higher rate of cell death during long-term culture as determined by real-time monitoring of propidium iodide (PI) staining (Fig. 2*C*).

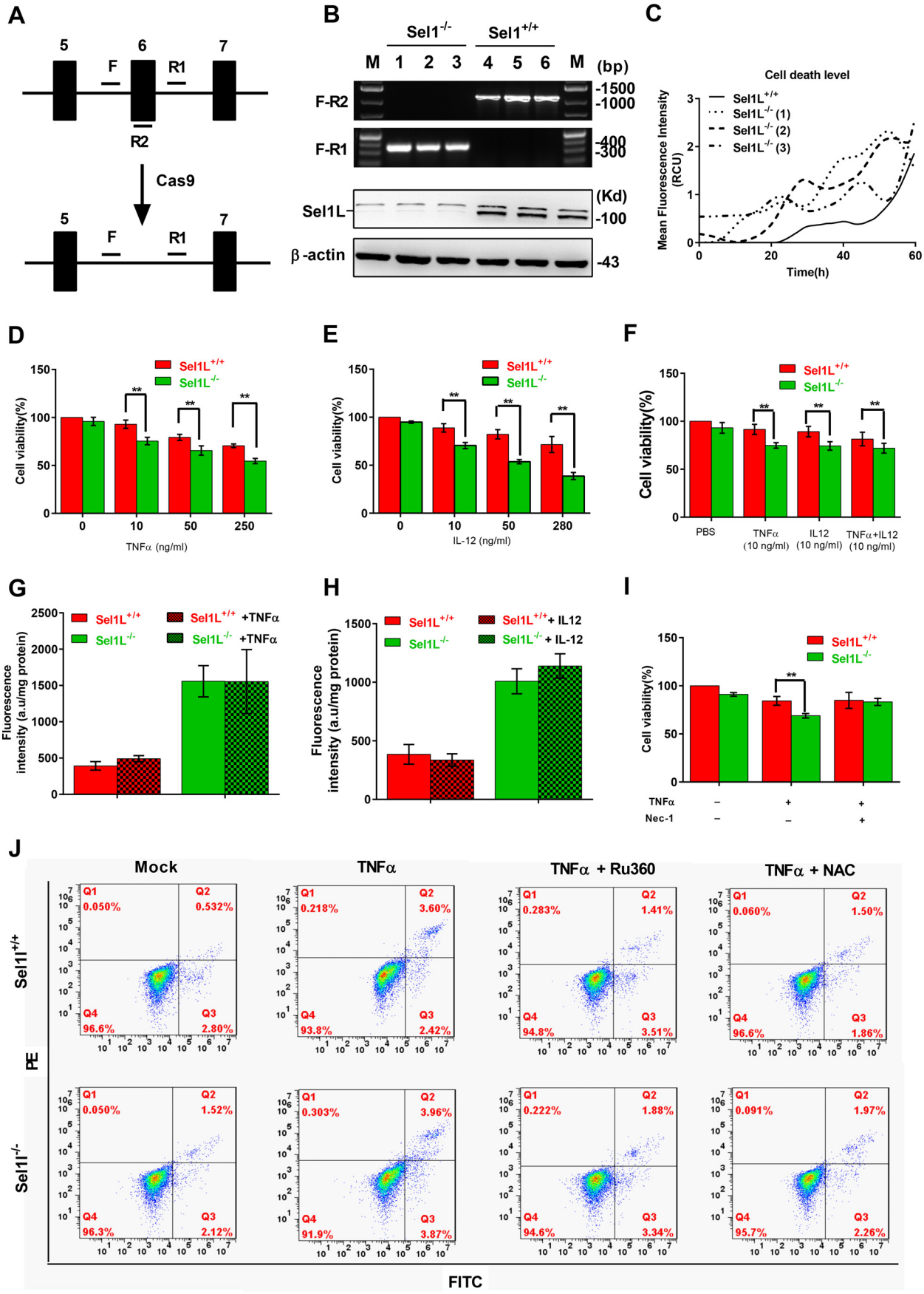
A
5
6
7
F
R1
R2
Cas9
5
F
R1
7
B
Sel1L-/-
Sel1L+/+
M 1 2 3 4 5 6 M (bp)
F-R2
-1500
-1000
F-R1
-400
-300
Sel1L
(Kd)
-100
β-actin
-43
C
Cell death level
Sel1L+/+
Sel1L-/- (1)
Sel1L-/- (2)
Sel1L-/- (3)
Mean Fluorescence Intensity (RCU)
Time(h)
D
Sel1L+/+
Sel1L-/-
Cell viability(%)
TNFα (ng/ml)
E
Sel1L+/+
Sel1L-/-
Cell viability(%)
IL-12 (ng/ml)
F
Sel1L+/+
Sel1L-/-
Cell viability(%)
PBS
TNFα (10 ng/ml)
IL12 (10 ng/ml)
TNFα+IL12 (10 ng/ml)
G
Sel1L+/+
Sel1L-/-
Sel1L+/+ +TNFα
Sel1L-/- +TNFα
Fluorescence intensity (a.u/mg protein)
H
Sel1L+/+
Sel1L-/-
Sel1L+/+ + IL12
Sel1L-/- + IL-12
Fluorescence intensity (a.u/mg protein)
I
Sel1L+/+
Sel1L-/-
Cell viability(%)
TNFα
Nec-1
J
Mock
TNFα
TNFα + Ru360
TNFα + NAC
Sel1l+/+
Sel1l-/-
PE
FITC
Q1 0.050% Q2 0.532% Q4 96.6% Q3 2.80%
Q1 0.218% Q2 3.60% Q4 93.8% Q3 2.42%
Q1 0.283% Q2 1.41% Q4 94.8% Q3 3.51%
Q1 0.060% Q2 1.50% Q4 96.6% Q3 1.86%
Q1 0.050% Q2 1.52% Q4 96.3% Q3 2.12%
Q1 0.303% Q2 3.96% Q4 91.9% Q3 3.87%
Q1 0.222% Q2 1.88% Q4 94.6% Q3 3.34%
Q1 0.091% Q2 1.97% Q4 95.7% Q3 2.26%

A number of pro-inflammatory cytokines promote cell death in diseases affecting the liver and other tissues. To assess whether ERAD deficiency exacerbates cytokine-mediated cell death, WT and SEL1L-deficient HepG2 cells were treated with the pro-inflammatory cytokines TNFα, IL-1α, IL-6, and IL-12) and followed by an assessment of cell viability by the MTT assay. SEL1L-deficient HepG2 cells suffered a higher level of cell death than WT HepG2 cells when incubated with doses as low as 10 ng/ml of either TNFα or IL-12 (Fig. 2, *D* and *E*, respectively). Incubation with both TNF-α and IL-12 did not yield a synergistic effect (Fig. 2*F*). In contrast, no difference in viability was observed between WT and SEL1L-deficient cells incubated with either IL-1α or IL-6 and IL-22 (Fig. S1).

Next we investigated possible mechanisms accounting for the increased susceptibility of SEL1L-deficient cells to the cell death promoting effects of TNFα and IL-12. We first monitored fluorescence in cells transfected with the ER stress reporter plasmid pCAX-F-XBPDBD-venus. As we have previously shown in other cells (15), SEL1L deficiency increased ER stress; more importantly, TNFα and IL-12 did not increase fluorescence in either WT or SEL1L-deficient cells (Fig. 2, *G* and *H*, respectively), ruling out a role of ER stress in mediating the effects of TNFα or IL-12. In contrast, incubation with the necrosis inhibitor necrostatin-1 (Nec-1) partially abolished the increased susceptibility of Sel1l$^{-/-}$ cells to the death-promoting effects of TNFα (Fig. 2*I*). Finally we used annexin V (FITC) and propidium iodide (PI) double dye-staining followed by FACS to ask whether NAC and Ru360 could correct the increased susceptibility of Sel1l$^{-/-}$ cells to TNFα. As shown in Fig. 2*J*, TNFα incubation induced a higher percentage of FITC/PE dual positive cells in Sel1l$^{-/-}$ than in WT population; more importantly, NAC or Ru360 significantly attenuated the death-promoting effects of TNFα. Overall, these results indicate that ERAD-deficient cells are more susceptible to the necrosis-promoting effects of TNFα and a portion of this increased susceptibility is accounted for by increased mitochondrial Ca^{2+} and ROS levels.

ERAD deficiency impairs mitochondrial morphology and cellular bioenergetics of HepG2 cells

Mitochondria were imaged using a green fluorescent reporter targeted to the mitochondrial outer membrane (15). Mitochondria of EerI-treated and SEL1L-deficient cells appeared more rounded than those in control cells (Fig. S2). To further determine the morphological changes of mitochondria induced by ERAD deficiency, we performed electron microscopic (EM) analysis for Sel1L$^{-/-}$ cells. Mitochondria in Sel1L$^{-/-}$ cells appeared more scarcely distributed with round and smaller shapes, compared with those in Sel1L$^{+/+}$ cells (Fig. 3, *A–D*). There were clear signs of mitochondrial fission (*arrowheads* in Fig. 3*D*) in Sel1L$^{-/-}$ cells. To assess whether these morphological changes were associated with altered function, we stained cells with the lipophilic cationic fluorescent dye JC-1 followed by dual channel FACS analysis. The ratio of high to low (H/L) fluorescence signals was substantially lower in Sel1L-deficient than in WT HepG2 cells indicating a reduction of mitochondrial membrane potential (MMP) in Sel1l$^{-/-}$ cells (Fig. S3*A*).

We next used Seahorse XF analysis to assess the effects of ERAD deficiency on cellular energetics. Sel1L-deficient cells showed an altered oxygen consumption rate (OCR) profile (Fig. S3*B*). The basal and maximal respiration rate, proton leak, and ATP production were significantly reduced (Fig. 3, *E–H*), whereas the spare respiratory capacity and nonmitochondrial respiration rate were not altered (Fig. 3, *I* and *J*). Conversely, extracellular acidification rate (ECAR), an index of glycolysis, did not differ between control and Sel1l$^{-/-}$ cells (Fig. S3*C*). Overall, these results suggest that ERAD-deficient cells suffer from a reduction of oxidative phosphorylation (OXPHOS), and as a consequence, reduced mitochondrial membrane potential.

ERAD deficiency promotes MOMP and sensitizes cells to proinflammatory cytokine-induced cell death

Next, we analyzed the effect of ERAD deficiency and TNF-α on the abundance and intracellular distributions of proteins involved in necrosis and apoptosis. Under basal conditions, whereas there was no difference between control and Sel1L-deficient HepG2 cells in the abundance total c-Jun N-terminal kinase (JNK), total cytochrome *c*, and receptor-interacting serine/threonine protein kinase 1 (RIPK1), but the latter had higher levels of phosphorylated p54 JNK (p54/*p*-JNK) and cytoplasmic cytochrome *c* (c-cytoochrome *c*) (Fig. 4, *A, left panels,* and *B* and *C*). Upon incubation with TNFα, p54/*p*-JNK, and C-cytochrome *c* contents in either cell types, but to a greater extent in Sel1L-deficient than in WT cells (Fig. 4, *A, middle panels*, and *B* and *C*), and this effect was attenuated by co-incubation with the JNK inhibitor SP600125 (Fig. 4, *A, right panels,* and *B* and *C*). Given the increased level of cytochrome *c* in the cytoplasm, we measured the activity of caspase 3 and 8. Consistent with the Western blotting result showing increased cytoplasmic content of cytochrome *c*, enzymatic analysis showed increased caspase 3 but not caspase 8 activity in Sel1l$^{-/-}$ HepG2 cells, and this pattern was exacerbated by treatment with TNFα (Fig. 4, *D* and *E*). Together, these data indicate that ERAD deficiency promotes MOMP leading to increased release of cytochrome *c*, and this process is exacerbated in the presence of the proinflammatory cytokine TNFα.

Figure 2. Genetic ablation of ERAD sensitizes HepG2 cells to TNFα– and IL-12–induced cell death. *A,* diagram illustrating CRISPR/Cas9-mediated editing of the Sel1L gene in HepG2 cells. *F, R1,* and *R2* represent PCR primers used for genotyping of Sel1L-edited cells. *Black bars* represent exons. *B*, *top*, PCR analysis of Sel1L-normal (Sel1L$^{+/+}$) and deleted (Sel1L$^{-/-}$) cells. *Bottom*, Western blotting analysis of SEL1L expression in Sel1L$^{+/+}$ and Sel1L$^{-/-}$ cells; the upper band is a nonspecific band. *C,* average cell death level of Sel1L$^{+/+}$ and Sel1L$^{-/-}$ cells as indicated by the mean PI fluorescence intensity. Sel1L$^{-/-}$ (*1-3*) represent three independent HepG2 cell clones. *D–F,* MTT assays of Sel1L$^{+/+}$ and Sel1L$^{-/-}$ cells after treatment with increased concentrations of TNF-α (*D*), IL-12 (*E*), and TNFα + IL-12 (*F*). *G* and *H,* fluorescence reporter assay of ER stress in TNF-α (*G*) and IL-12 (*H*) treated Sel1L$^{+/+}$ and Sel1L$^{-/-}$ cells. *I,* MTT assay of Sel1L$^{+/+}$ and Sel1L$^{-/-}$ cells after treatment with TNFα or TNFα + Nec-1. *J*, FITC and PE dual channel FACS assay of Sel1L$^{+/+}$ and Sel1L$^{-/-}$ cells after treatment with PBS (Mock), TNF-α, TNF-α + Ru360, or TNF-α + NAC. All data are mean ± S.E. ($n = 3$). *, $p < 0.05$; **, $p < 0.01$ by Student's *t* test.

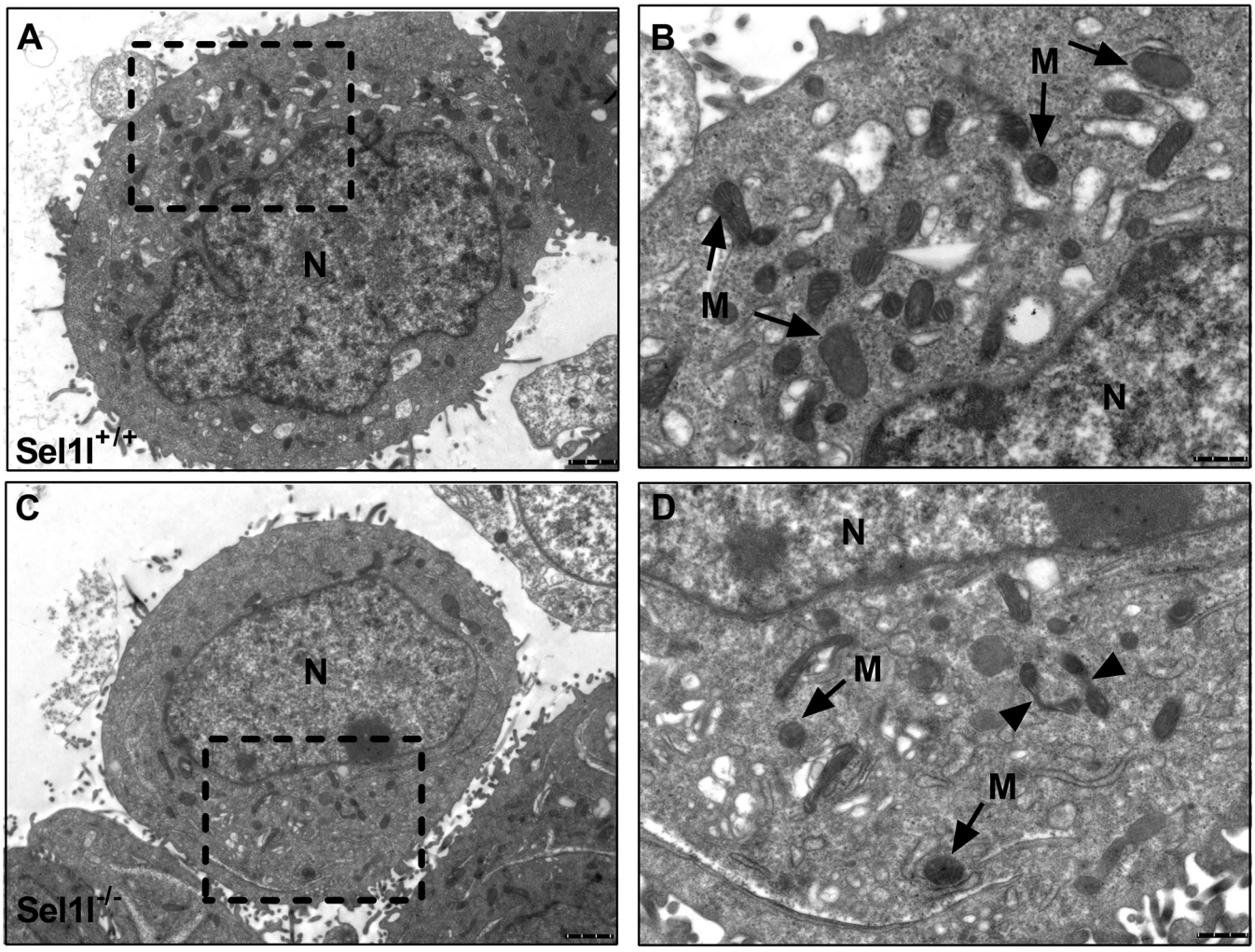
A
N
Sel1l+/+
B
M
M
N
C
N
Sel1l-/-
D
N
M
M

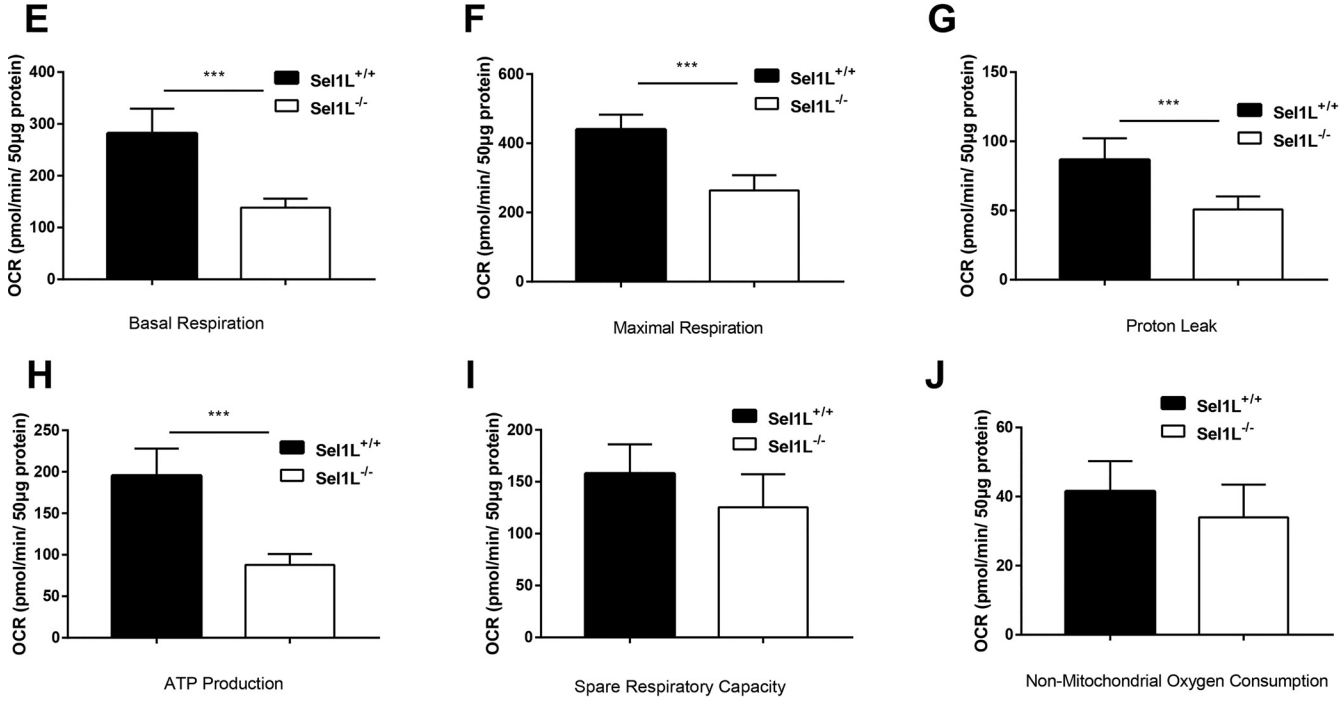
E
OCR (pmol/min/ 50µg protein)
400
300
200
100
0
***
Sel1L+/+
Sel1L-/-
Basal Respiration
F
OCR (pmol/min/ 50µg protein)
600
400
200
0
***
Sel1L+/+
Sel1L-/-
Maximal Respiration
G
OCR (pmol/min/ 50µg protein)
150
100
50
0
***
Sel1L+/+
Sel1L-/-
Proton Leak
H
OCR (pmol/min/ 50µg protein)
250
200
150
100
50
0
***
Sel1L+/+
Sel1L-/-
ATP Production
I
OCR (pmol/min/ 50µg protein)
200
150
100
50
0
Sel1L+/+
Sel1L-/-
Spare Respiratory Capacity
J
OCR (pmol/min/ 50µg protein)
60
40
20
0
Sel1L+/+
Sel1L-/-
Non-Mitochondrial Oxygen Consumption

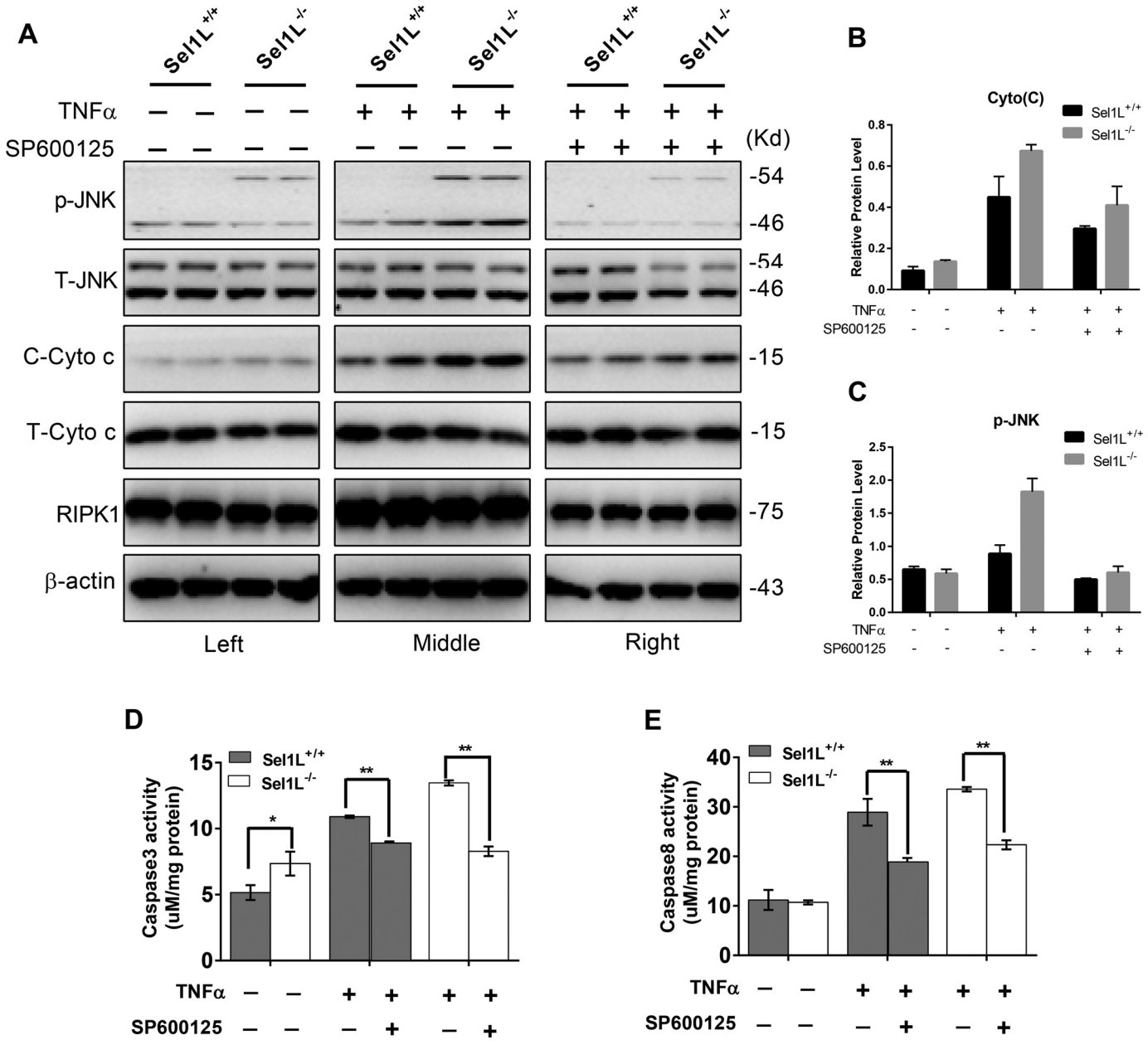

Figure 4. ERAD deficiency induces increased mitochondrial outer membrane permeability and activation of apoptosis. *A,* Western blotting analysis of RIPK1, total and cytoplasmic cytochrome *c* (*T-* and *C-cyto c*), total and phosphorylated JNK (*T-* and *p-JNK*) in Sel1L$^{+/+}$ and Sel1L$^{-/-}$ cells treated with TNF-α or TNF-α + SP600125. *β*-Actin was used as a loading control. *B* and *C,* quantification of cytoplasmic cytochrome *c* (*B*) and phosphorylated JNK (C) in Sel1L$^{+/+}$ and Sel1L$^{-/-}$ cells following TNFα or TNFα + SP600125 treatment. *D* and *E,* ELISA analysis of caspase 3 (*D*) and caspase 8 (*E*) activity in TNF-α or TNF-α + SP600125-treated Sel1L$^{+/+}$ and Sel1L$^{-/-}$ cells. Data are mean ± S.E. ($n = 3$). *, $p < 0.05$; **, $p < 0.01$ by Student's *t* test.

ERAD deficiency causes transcriptional rewiring that disrupts multiple mitochondrial activities but activates several pathways related to "stemness" property of cells

Finally, we used RNA-Seq on WT and ERAD-deficient cells to obtain a global view of the consequences of ERAD deficiency on gene expression. This analysis identified 1216 differentially expressed genes (DEGs), including 199 up-regulated and 1017 down-regulated genes. By gene enrichment analysis for the Gene Ontology biological process and biological pathway, the down-regulated DEGs were found to be significantly enriched in the functional categories including mitochondrial structure and function (mitochondrial ATP synthesis coupled electron transport, mitochondrion organization, mitochondrial respiratory chain complex assembly, mitochondrial translation, and mitochondrial transmembrane transport), endoplasmic reticulum function (protein targeting to ER and establishment of

Figure 3. ERAD deficiency alters the morphology and function of mitochondria in HepG2 cells. *A* and *C,* electron microscopic images of Sel1L$^{+/+}$ (*A*) and Sel1L$^{-/-}$ (*C*) cells. *B* and *D,* magnified view of the *dash line* marked region in *A* and *C*, respectively. *N,* nucleus; *M,* mitochondria. *Arrowheads* in *D* indicate sites of mitochondrial fission. *E–J,* quantification of basal (*E*) and maximal (*F*) respiration, proton leak (*G*), ATP production (*H*), spare respiration capacity (*I*), and nonmitochondrial oxygen consumption (*J*) of Sel1L$^{+/+}$ and Sel1L$^{-/-}$ cells. Data are mean ± S.E. ($n = 3$). *, $p < 0.05$; **, $p < 0.01$ by Student's *t* test.

protein localization to endoplasmic reticulum), and metabolic process related to mitochondria or endoplasmic reticulum (oxidative phosphorylation, respiratory electron transport, oxidation−reduction process, and metabolic pathways) (Fig. 5, *A, left*, and *B*). The up-regulated genes were overrepresented in epithelial cell adhesion, P53 signaling, MAPK signaling, mitochondrial structure and function (mitochondrial fragmentation, negative regulation of mitochondrial Ca^{2+} concentration, regulation of Ca^{2+} import, Ca^{2+} channels), endoplasmic reticulum function (protein exit from the ER, protein processing in the ER, unfolded protein response) (Fig. 5, *A, right*, and *C*). Overall, these results indicate that ERAD deficiency caused a global reorganization of mitochondrial activities.

To further understand the pathophysiological significance of the obtained molecular signature in ERAD-deficient HepG2 cells, we performed gene set enrichment analysis (GSEA) by comparing the identified DEGs to *a priori*-established gene modules. As expected, genes of a reported mitochondrial gene module (16) were overrepresented in the down-regulated DEGs in ERAD-deficient HepG2 cells (Fig. 5*D*). Intriguingly, the Jak2 signaling pathway-associated or the so-called stemness genes (17, 18) were highly represented in the up-regulated DEGs (Fig. 5*E*). Together, these results indicate that ERAD deficiency caused a global reorganization of transcription that disrupts multiple mitochondrial activities and activates several pathways associated with the stemness or invasiveness property of eukaryotic cells.

Discussion

The endoplasmic reticulum and mitochondria are physically and functionally integrated with each other to coordinate an array of metabolic and biosynthetic functions. It has been shown recently that ER protein quality control or ERAD affects mitochondrial dynamics in brown adipose cells by regulating the turnover of the MAM protein, sigma receptor 1 (SigmaR1) (19). Stress or dysfunction in one compartment is likely to affect the other and the overall function status of the cell. Here, we provide evidence that ERAD deficiency impacts mitochondrial function human hepatic cells via influencing their Ca^{2+} and ROS homeostasis. We show that pharmacological inhibition or genetic disruption of ERAD function decrease the viability of hepatic cell line HepG2 and sensitize them to TNF-α–induced cell death. ERAD deficiency induces Ca^{2+} overflow from the ER to mitochondria, causing over-production of ROS and subsequent damage to the mitochondrial outer membrane. ERAD-deficient cells had decreased ATP production, reduced mitochondrial transmembrane potential, and increased outer membrane permeability and most notably, transcriptome analysis indicates that ERAD deficiency caused a global reorganization of the transcription program. These results highlight an important role for ERAD in maintaining mitochondrial health and cell survival by, at least partially, supporting mitochondrial Ca^{2+} and ROS homeostasis.

Increasing evidence links ER stress to the development of chronic human diseases, such as type 2 diabetes mellitus, NAFLD, neurodegeneration, and cancer (1–3). However, the mechanisms whereby ER stress lead to the pathogenesis of various human diseases are incompletely understood. ER stress has been shown to activate the unfolded protein response (UPR) responses or the CHOP-dependent cell death program (5, 6). However, this current UPR model alone cannot fully explain why ER stress preferentially affects metabolically active organs, such as neurons, the endocrine pancreas and liver.[4] In this study, we show that chronic ER stress due to defective ERAD causes structural and functional damages to mitochondria. Moreover, we demonstrate that blocking mitochondria Ca^{2+} uptake or removing excessive ROS partially rescues cellular defects of ERAD-deficient cells. Given the essential roles of mitochondria in regulating cellular physiology, metabolism, and cell death (20), our results suggest that mitochondrial dysfunction may be an under-appreciated driver of many ER stress-induced pathogenesis. These results also strongly support an increasingly recognized notion that normal cellular and organismal health depends on tightly regulated inter-organelle interaction and communication, particularly under stressed conditions, such as viral infection or obesity (21).

Our results provide some mechanistic evidence to explain how ERAD deficiency leads to mitochondrial dysfunction. The ER makes contact with mitochondria through the formation of MAMs, which are temporary structures required for exchange of Ca^{2+} and other molecules between these two organelles (22). We showed that, first, elevated levels of Ca^{2+} and ROS were detected in mitochondria of EerI-treated and SEL1L-depleted HepG2 cells. Second, blocking mitochondria Ca^{2+} uptake by treating ERAD-deficient HepG2 cells with Ru360 (a known MCU inhibitor), or removing excessive mitochondrial ROS with NAC (a mitochondria ROS scavenger), partially restores mitochondrial function of ERAD-deficient HepG2 cells. Furthermore, increased cytochrome *c*, a mitochondrial matrix protein, was detected in the cytoplasmic compartment of ERAD-deficient HepG2 cells. These results suggest a model whereby ERAD deficiency triggers overflow of Ca^{2+} from the ER to mitochondria, which in turn enhances ROS production and progressive damage to the mitochondrial respiratory system and membrane structure.

Cell death is a common histological feature of many chronic diseases, and inflammatory cytokines have been shown to play an important role during this process (23). For example, the pro-inflammatory cytokine TNF-α contributes to the development and progression of inflammation-related diseases, such as nonalcohol steatohepatitis, type 2 diabetes, and cancer, by promoting necrotic cell death (24–26). Importantly, we show that TNF-α–induced cell death is increased in the nascence of ERAD and that this effect could be blocked with the necrosis inhibitor Nec-1. These results indicate that ERAD deficiency exacerbates the cell death-promoting effect of TNFα. Although further studies are needed to clarify the exact molecular mechanisms underlying the observed synergy between ERAD deficiency and TNF-α on cell death, we speculate that the lower intracellular ATP level, the impaired mitochondrial Ca^{2+} level and increased mitochondrial outer membrane permeability may be among the contributing factors.

[4] Q. Long et al., unpublished data.

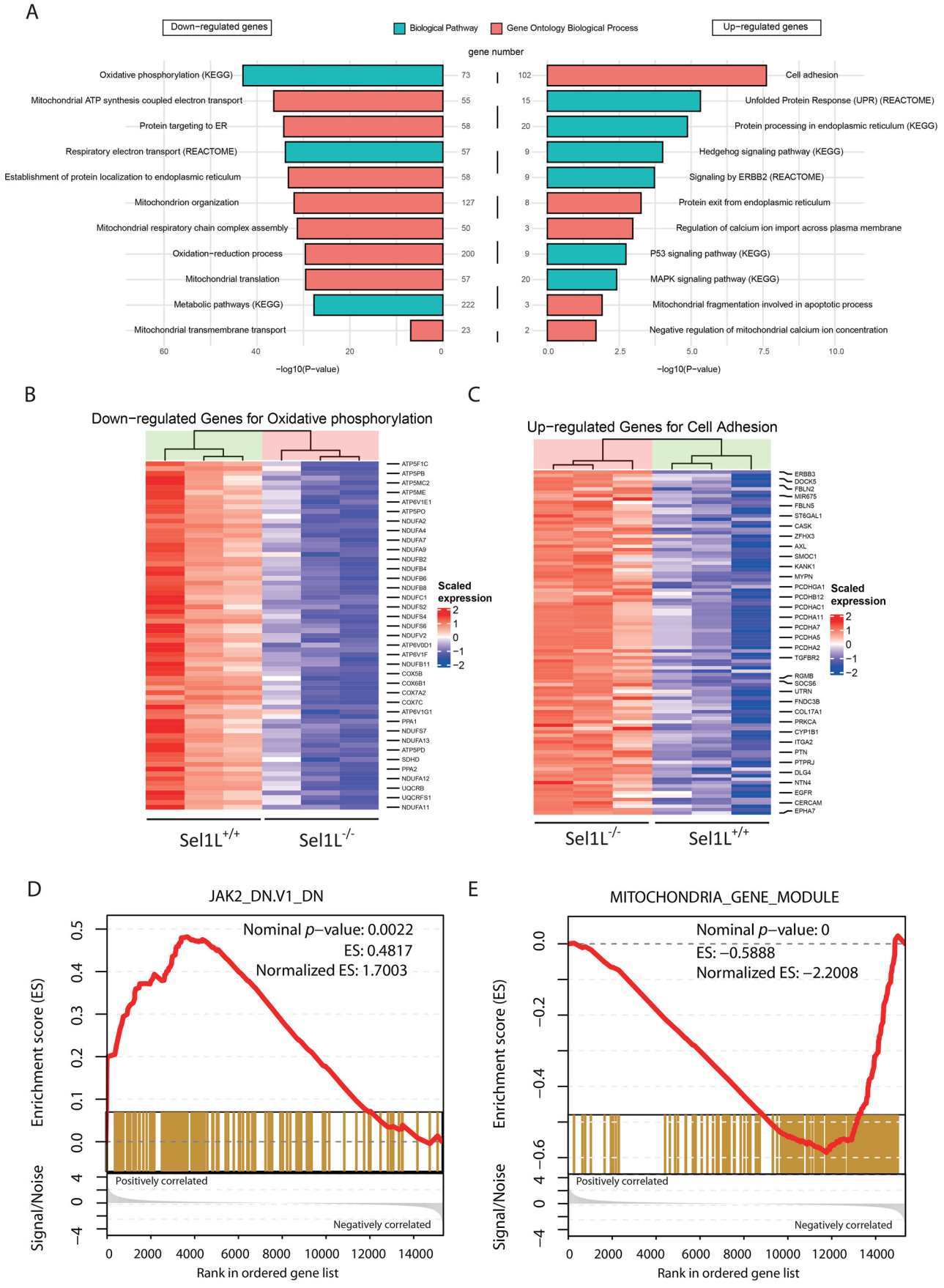
A
Down−regulated genes
Biological Pathway
Gene Ontology Biological Process
Up−regulated genes
gene number
Oxidative phosphorylation (KEGG)
Mitochondrial ATP synthesis coupled electron transport
Protein targeting to ER
Respiratory electron transport (REACTOME)
Establishment of protein localization to endoplasmic reticulum
Mitochondrion organization
Mitochondrial respiratory chain complex assembly
Oxidation−reduction process
Mitochondrial translation
Metabolic pathways (KEGG)
Mitochondrial transmembrane transport
73
55
58
57
58
127
50
200
57
222
23
Cell adhesion
Unfolded Protein Response (UPR) (REACTOME)
Protein processing in endoplasmic reticulum (KEGG)
Hedgehog signaling pathway (KEGG)
Signaling by ERBB2 (REACTOME)
Protein exit from endoplasmic reticulum
Regulation of calcium ion import across plasma membrane
P53 signaling pathway (KEGG)
MAPK signaling pathway (KEGG)
Mitochondrial fragmentation involved in apoptotic process
Negative regulation of mitochondrial calcium ion concentration
102
15
20
9
9
8
3
9
20
3
2
−log10(P−value)
−log10(P−value)
B
Down−regulated Genes for Oxidative phosphorylation
Scaled expression
Sel1L+/+
Sel1L−/−
C
Up−regulated Genes for Cell Adhesion
Scaled expression
Sel1L−/−
Sel1L+/+
D
JAK2_DN.V1_DN
Nominal p−value: 0.0022
ES: 0.4817
Normalized ES: 1.7003
Enrichment score (ES)
Signal/Noise
Positively correlated
Negatively correlated
Rank in ordered gene list
E
MITOCHONDRIA_GENE_MODULE
Nominal p−value: 0
ES: −0.5888
Normalized ES: −2.2008
Enrichment score (ES)
Signal/Noise
Positively correlated
Negatively correlated
Rank in ordered gene list

ERAD deficiency had profound effects on gene expression in HepG2 cells. RNA-Seq revealed over 1200 DEGs in ERAD-deficient cells with the majority falling in the category of down-regulated genes. Many of those genes are involved in OXPHOS, ATP synthesis, mitochondrial organization, and respiratory chain complex assembly (Fig. 5*A*). It is possible that down-regulation of these genes are a consequence of the activation of the mitochondrial unfolded protein response (UPR^{mt}) (27). A major outcome of the activation of the UPR^{mt} pathway is suppression of the transcription of mitochondrial function-associated genes, so that the overall mitochondrial activity would be tuned down to reduce mitochondrial stress (28). However, many mitochondrial organization and respiratory chain complex assembly are also down-regulated in ERAD-deficient HepG2 cells. A possible explanation for the down-regulation of these genes is that the damage of mitochondria in ERAD-deficient cells has reached a threshold point of "no-return," so that a mitochondrial functional collapse had occurred.

Intriguingly, most of the 200 up-regulated genes in Sel1L-deficient cells are associated with either cell adhesion or proliferation. Gene set enrichment analysis showed that these genes overlap significantly with a group of so-called stemness genes in the IL-6/STAT3 signaling pathway (17, 18). Although further studies are needed to ascertain whether the ERAD-deficient HepG2 cells have reverted to stem-like or more aggressive cells, these results provide evidence that ERAD deficiency may potentiate mammalian cells toward stem or cancer-like cells, perhaps through influencing their mitochondrial function.

In summary, we demonstrate here that ERAD deficiency decrease the viability of HepG2 cells and sensitizes them to TNFα-induced cell death. ERAD deficiency also enhances the stemness or metastasis property of mammalian cells. Mechanistically, ERAD deficiency induces structural and functional damage of mitochondria by impairing the ability of mitochondrial to maintain Ca^{2+} and ROS homeostasis. Our findings highlight the importance of a regulated ER-mitochondria interaction in supporting normal cellular and organismal physiology, and have important implications in understanding the molecular mechanisms of chronic diseases, such as T2D, nonalcohol steatohepatitis, neurodegeneration, and cancer.

Materials and methods

Cell culture, plasmid transfection, fluorescent imaging, and CRISPR/Cas9 mediated gene editing

HepG2 cells were cultured in Dulbecco's modified Eagle's medium supplemented with 15% fetal bovine serum, 100 units/ml of penicilin,100 μg/ml of streptomycin at 37 °C in an humidified CO_2 incubator. For visualization of mitochondria or monitoring ER stress, the expression plasmids *p*-mtGFP containing mitochondria-targeted GFP, or pCAX-F-XBPDBD-venus (29) were transfected into HepG2 cells using Lipofectamine 3000. GFP images were acquired with a Fluoview FV1000 Olympus confocal microscope analyzed by the software Image J (NIH Image).

For Cas9-mediated gene editing, sgRNAs flanking exon 6 were designed using the Optimized CRISPR Design tool (https://www.synthego.com/products/bioinformatics/crispr-design-tool) and cloned into the expression vector pGL3-U6-2sgRNA. To generate SEL1L-deficient HepG2 cell lines, the sgRNA expression vector and the Cas9 expression plasmid pST1374-NLS-3xFlag-linker-Cas9 (30) were co-transfected into HepG2 cells using Lipofectamine 3000. After transfection, puromycin (5 μg/ml) was added to the culture medium to select for puromycin-resistant cells. A week later, puromycin-resistant HepG2 colonies were picked, expanded, and analyzed by PCR using primers F (−3′ R1 (5′-GCCTTTT-GGAGATACCGATATG) flanking exon 6 and exon 6-specific primer R2 (5′-GGCAGAGACTGGAGTGCTCACT).

Cell death and viability assay

WT and Sel1L-deficient HepG2 cells were seeded into a 6-well–plate at an initial density of 1×10^5/well and allowed to recover for 12 h. PI and annexin V were then added into the culture medium (10 ng/ml) and cell death was monitored in real-time over the next 72 h using an Incucyte Zoom system. Cell viability was assessed by MTT assay or by FACS using a Beckman Counter Flow Cytometer.

ROS, cytosolic and mitochondrial Ca^{2+} measurement

HepG2 cells were seeded into 4-well glass-bottomed chambers (Nunc, IL) at a density of 1×10^5/well in Dulbecco's modified Eagle's medium and cultured for 24 h. Cytosolic and mitochondrial Ca^{2+} and intracellular ROS were measured by adding the freshly prepared fluorescent dye Fluo4/AM, Rhod2 AM (Invitrogen), and Mitosox into the culture medium followed by cell imaging with a Fluoview FV1000 Olympus confocal microscope.

Mitochondrial transmembrane potential, OXPHOS, and glycolytic functional analysis

Mitochondrial transmembrane potential was determined using a JC-1 mitochondrial membrane potential assay kit (Abcam). Oxidative phosphorylation and glycolysis were determined using a Seahorse XFe24 extracellular flux analyzer (Seahorse Bioscience) according to the manufacturer's protocols and as previously described (31). Briefly, a total of 4×10^4 cells were seeded in each well of Seahorse XF24 cell culture microplate and cultured for 16 h in complete medium. The OCR and ECAR were assayed using the XF Cell Mito Stress Test Kit and

Figure 5. ERAD deficiency causes overhauling of mitochondrial activities and enhances the stemness property of HepG2 cells. $Sel1L^{+/+}$ and $Sel1L^{-/-}$ cells were seeded at 1×10^5/well in 6-well–plates and cultured in a humidified CO_2 incubator for 36 h before being subjected to total RNA extraction using the TRIzol kit. Three replicates of RNA sample for each genotype were used for RNA-Seq. *A,* Gene Ontology biological process (*red*) and biological pathways enrichment (*green*) analysis of down-regulated (*left*) and up-regulated (*right*) genes in $Sel1L^{-/-}$ cells. *B* and *C,* representative heatmaps of down-regulated (*B*) and up-regulated (*C*) genes in $Sel1L^{-/-}$ cells. *Colors* indicate scaled expression of individual genes. *D* and *E,* gene set enrichment plot of down-regulated (*D*) and up-regulated (*E*) genes in $Sel1L^{-/-}$ cells. The reference gene modules used in *D* and *E* are the Wong mitochondria gene module (https://www.gsea-msigdb.org/gsea/msigdb/cards/WONG_MITOCHONDRIA_GENE_MODULE) and the JAK2 pathway module (https://www.gsea-msigdb.org/gsea/msigdb/cards/JAK2_DN.V1_DN), respectively. Each *vertical bar* on the *x* axis in *D* and *E* represents a denoted gene in the specific gene set.

XF Glycolysis Stress Test Kit, respectively, coupled with the XF24-3 Extracellular Flux Assay Kit. All OCR and ECAR measurements were normalized to protein content.

Western blotting and probing

Protein isolation, gel electrophoresis, and blotting were performed essentially as described (15). After blocking with 5% skim milk, membranes were incubated at 4 °C overnight with primary antibodies aginst: *p*-JNK (Santa Cruz, 1:800), Caspase-1 (Santa Cruz, 1:800), JNK1 (Santa Cruz, 1:800), RIPK1 (Affinity, 1:1000), Cytc (CST, 1:1000), MCU (Sigma, 1:800), and β-actin (Sigma, 1:1000). Signals were developed by incubating with 1/5000-fold dilution of anti-rabbit or anti-mouse secondary antibodies for 1 h at room temperature and quantified using the Image Laboratory Software on a ChemiDoc XRS system (Bio-Rad).

RNA-Seq and bioinformatics analyses

Total RNA was isolated from HepG2 cells grown under standard conditions using TRIzol reagent (Invitrogen). RNA-Seq was performed by GENEWIZ Co., Ltd. (Suzhou, China). In brief, libraries were prepared using the VAHTS mRNA-seq V2 Library Prep Kit for Illumina, according to the manufacturers' instructions. Sequencing libraries were run on an Illumina NovaSeq platform with the 2× 150-bp paired-end protocol. These RNA-Seq data has been deposited onto public repository of Genome Sequence Archive (GSA) database in BIG Data Center (BioProject: PRJCA002400; GSA accession number: CRA002460).

Raw reads yielded by paired-end transcriptome sequencing were mapped to the human reference genome (GRCh37/hg19) by tophat2 (version 2.1.1) (32). Read counts were obtained from BAM files using samtools (version 1.9) and gfold (version 1.1.4) (33), and then converted into log2 counts/million (logCPM) values to quantify the gene expression level by the R package edgeR (version 3.26.8) (34). Statistical significances of differentially expressed genes were determined by the empirical Bayes method powered by the R package limma (version 3.40.6) (35) with $p < 0.005$ as the statistical cutoff. Programs written in R language (version 3.6.1) use library extension to pull in functions from noncore packages from the bioconductor repository (RRID:SCR_006442).

ToppGene Suite (RRID:SCR_005726) (36) was used to perform the enrichment analysis of differentially expressed genes for Gene Ontology (GO) biological process (Gene_Ontology_Consortium, 2015), Reactome pathway (37), and Kyoto Encyclopedia of Genes and Genomes (KEGG) pathway (38). GSEA (version 4.0.3) (39) was performed to identify the *a priori* defined gene set associated with transcriptome differences between phenotype (*SEL1L*-deficient *versus* intact WT). The c6.all.v7.0.symbols.gmt (oncogenic signatures) and c2.cgp.v7.0.symbols.gmt (chemical and genetic perturbations) gene set libraries were used as the reference gene set collection for enrichment analysis. The statistical cutoff for this analysis was set at $p < 0.05$.

Statistical analyses

Data were analyzed by Student's *t* test or two-way repeated analysis of variance using GraphPad (7.0) with statistical significance set at $p < 0.05$. Data are present as mean ± S.E.

Data availability

High-throughput sequencing data for HepG2 cells are stored in the BioProject Library (https://bigd.big.ac.cn/bioproject/browse/PRJCA002400). All other data are contained within the manuscript.

Acknowledgments—We thank Yuanyuan Gao, Jiaojiao Sun, and Wenyan Ren for technical assistance; Drs. Masayuki Miura, Ying Xu, and Han Wang for expression plasmids or other reagents; Dr. Wensheng Zhang for helpful discussions and critical comments on the manuscript.

Author contributions—Q. Liu, G. L., and Y. H. investigation; Q. Liu, G. L., and Y. H. methodology; X. Y. data curation; X. Y. software; Z. G. resources; Z. G. and Y. R. B. supervision; Y. R. B. and Q. Long writing-review and editing; Q. Long conceptualization; Q. Long funding acquisition; Q. Long writing-original draft.

Funding and additional information—This work was supported by the National Key R&D Program of China Grant 2019YFA0802400 and Natural Science Foundation of China Grant 31571489 (to Q. M. L.).

Conflict of interest—The authors declare that they have no conflicts of interest with the contents of this article.

Abbreviations—The abbreviations used are: ER, endoplasmic reticulum; ERAD, endoplasmic reticulum-associated degradation; NAFLD, nonalcohol fatty liver disease; UPR, unfolded protein response; CHOP, CCAAT-enhancer-binding protein homologous protein; MAM, mitochondria-associated membrane; MOMP, mitochondrial outer membrane permeability; TNF-α, tumor necrosis factor α; EerI, eeyarestatin I; RR, ruthenium red; ROS, reactive oxygen species; NAC, *N*-acetylcysteine; PI, propidium iodide; IL, interleukin; PE, phosphatidylethanolamine; OCR, oxygen consumption rate; ECAR, extracellular acidification rate; OXPHOS, oxidative phosphorylation; JNK, c-Jun N-terminal kinase; RIPK1, receptor-interacting serine/threonine protein kinase 1; DEG, differentially expressed gene; GSEA, gene set enrichment analysis; MTT, 3-(4,5-dimethylthiazol-2-yl)-2,5-diphenyltetrazolium bromide.

References

1. Moon, H. W., Han, H. G., and Jeon, Y. J. (2018) Protein quality control in the endoplasmic reticulum and cancer. *Int. J. Mol. Sci.* **19,** 3020 CrossRef
2. Kim, J. Y., Garcia-Carbonell, R., Yamachika, S., Zhao, P., Dhar, D., Loomba, R., Kaufman, R. J., Saltiel, A. R., and Karin, M. (2018) ER stress drives lipogenesis and steatohepatitis via caspase-2 activation of S1P. *Cell* **175,** 133–145e115 CrossRef Medline
3. Zhu, B., Jiang, L., Huang, T., Zhao, Y., Liu, T., Zhong, Y., Li, X., Campos, A., Pomeroy, K., Masliah, E., Zhang, D., and Xu, H. (2017) ER-associated degradation regulates Alzheimer's amyloid pathology and memory function by modulating γ-secretase activity. *Nat. Commun.* **8,** 1472 CrossRef Medline

4. Malhi, H., and Kaufman, R. J. (2011) Endoplasmic reticulum stress in liver disease. *J. Hepatol.* **54,** 795–809 CrossRef Medline
5. Yoshida, H., Matsui, T., Hosokawa, N., Kaufman, R. J., Nagata, K., and Mori, K. (2003) A time-dependent phase shift in the mammalian unfolded protein response. *Dev. Cell* **4,** 265–271 CrossRef Medline
6. Rao, J., Zhang, C., Wang, P., Lu, L., Qian, X., Qin, J., Pan, X., Li, G., Wang, X., and Zhang, F. (2015) C/EBP homologous protein (CHOP) contributes to hepatocyte death via the promotion of ERO1α signalling in acute liver failure. *Biochem. J.* **466,** 369–378 CrossRef Medline
7. Sironi, L., Restelli, L. M., Tolnay, M., Neutzner, A., and Frank, S. (2020) Dysregulated interorganellar crosstalk of mitochondria in the pathogenesis of Parkinson's disease. *Cells* **9,** 233 CrossRef
8. Dimmer, K. S., and Scorrano, L. (2006) (De)constructing mitochondria: what for? *Physiology (Bethesda)* **21,** 233–241 CrossRef Medline
9. Vafai, S. B., and Mootha, V. K. (2012) Mitochondrial disorders as windows into an ancient organelle. *Nature* **491,** 374–383 CrossRef Medline
10. Bohovych, I., and Khalimonchuk, O. (2016) Sending out an SOS: mitochondria as a signaling hub. *Front. Cell Dev. Biol.* **4,** 109 CrossRef Medline
11. Naon, D., and Scorrano, L. (2014) At the right distance: ER-mitochondria juxtaposition in cell life and death. *Biochim. Biophys. Acta* **1843,** 2184–2194 CrossRef Medline
12. Gomez-Suaga, P., Paillusson, S., and Miller, C. C. J. (2017) ER-mitochondria signaling regulates autophagy. *Autophagy* **13,** 1250–1251 CrossRef Medline
13. Filadi, R., Greotti, E., Turacchio, G., Luini, A., Pozzan, T., and Pizzo, P. (2015) Mitofusin 2 ablation increases endoplasmic reticulum-mitochondria coupling. *Proc. Natl. Acad. Sci. U.S.A.* **112,** E2174–2181 CrossRef Medline
14. Kornmann, B., Currie, E., Collins, S. R., Schuldiner, M., Nunnari, J., Weissman, J. S., and Walter, P. (2009) An ER-mitochondria tethering complex revealed by a synthetic biology screen. *Science* **325,** 477–481 CrossRef Medline
15. Hu, Y., Gao, Y., Zhang, M., Deng, K. Y., Singh, R., Tian, Q., Gong, Y., Pan, Z., Liu, Q., Boisclair, Y. R., and Long, Q. (2019) Endoplasmic reticulum-associated degradation (ERAD) has a critical role in supporting glucose-stimulated insulin secretion in pancreatic β-cells. *Diabetes* **68,** 733–746 CrossRef Medline
16. Wong, D. J., Nuyten, D. S., Regev, A., Lin, M., Adler, A. S., Segal, E., van de Vijver, M. J., and Chang, H. Y. (2008) Revealing targeted therapy for human cancer by gene module maps. *Cancer Res.* **68,** 369–378 CrossRef Medline
17. Abubaker, K., Luwor, R. B., Zhu, H., McNally, O., Quinn, M. A., Burns, C. J., Thompson, E. W., Findlay, J. K., and Ahmed, N. (2014) Inhibition of the JAK2/STAT3 pathway in ovarian cancer results in the loss of cancer stem cell-like characteristics and a reduced tumor burden. *BMC Cancer* **14,** 317 CrossRef Medline
18. Neradugomma, N. K., Subramaniam, D., Tawfik, O. W., Goffin, V., Kumar, T. R., Jensen, R. A., and Anant, S. (2014) Prolactin signaling enhances colon cancer stemness by modulating Notch signaling in a Jak2-STAT3/ERK manner. *Carcinogenesis* **35,** 795–806 CrossRef Medline
19. Zhou, Z., Torres, M., Sha, H., Halbrook, C. J., Van den Bergh, F., Reinert, R. B., Yamada, T., Wang, S., Luo, Y., Hunter, A. H., Wang, C., Sanderson, T. H., Liu, M., Taylor, A., Sesaki, H., *et al.* (2020) Endoplasmic reticulum-associated degradation regulates mitochondrial dynamics in brown adipocytes. *Science* **368,** 54–60 CrossRef Medline
20. Nunnari, J., and Suomalainen, A. (2012) Mitochondria: in sickness and in health. *Cell* **148,** 1145–1159 CrossRef Medline
21. Sargsyan, Y., and Thoms, S. (2020) Staying in healthy contact: how peroxisomes interact with other cell organelles. *Trends Mol. Med.* **26,** 201–214 CrossRef Medline
22. Filadi, R., Theurey, P., and Pizzo, P. (2017) The endoplasmic reticulum-mitochondria coupling in health and disease: molecules, functions and significance. *Cell Calcium* **62,** 1–15 CrossRef Medline
23. Duvigneau, J. C., Luís, A., Gorman, A. M., Samali, A., Kaltenecker, D., Moriggl, R., and Kozlov, A. V. (2019) Crosstalk between inflammatory mediators and endoplasmic reticulum stress in liver diseases. *Cytokine* **124,** 154577 CrossRef Medline
24. Shuh, M., Bohorquez, H., Loss, G. E., Jr., and Cohen, A. J. (2013) Tumor necrosis factor-α: life and death of hepatocytes during liver ischemia/reperfusion Injury. *Ochsner J.* **13,** 119–130 Medline Medline
25. Montgomery, S. L., and Bowers, W. J. (2012) Tumor necrosis factor-alpha and the roles it plays in homeostatic and degenerative processes within the central nervous system. *J. Neuroimmune Pharmacol.* **7,** 42–59 CrossRef Medline
26. Walczak, H. (2011) TNF and ubiquitin at the crossroads of gene activation, cell death, inflammation, and cancer. *Immunol. Rev.* **244,** 9–28 CrossRef Medline
27. Shpilka, T., and Haynes, C. M. (2018) The mitochondrial UPR: mechanisms, physiological functions and implications in ageing. *Nat. Rev. Mol. Cell Biol.* **19,** 109–120 CrossRef Medline
28. Melber, A., and Haynes, C. M. (2018) UPR(mt) regulation and output: a stress response mediated by mitochondrial-nuclear communication. *Cell Res.* **28,** 281–295 CrossRef Medline
29. Iwawaki, T., Akai, R., Kohno, K., and Miura, M. (2004) A transgenic mouse model for monitoring endoplasmic reticulum stress. *Nat. Med.* **10,** 98–102 CrossRef Medline
30. Baillat, D., Russell, W. K., and Wagner, E. J. (2016) CRISPR-Cas9 mediated genetic engineering for the purification of the endogenous integrator complex from mammalian cells. *Protein Expr. Purif.* **128,** 101–108 CrossRef Medline
31. Zhu, P., Liu, Y., Zhang, F., Bai, X., Chen, Z., Shangguan, F., Zhang, B., Zhang, L., Chen, Q., Xie, D., Lan, L., Xue, X., Liang, X. J., Lu, B., Wei, T., *et al.* (2018) Human elongation factor 4 regulates cancer bioenergetics by acting as a mitochondrial translation switch. *Cancer Res.* **78,** 2813–2824 CrossRef Medline
32. Kim, D., Pertea, G., Trapnell, C., Pimentel, H., Kelley, R., and Salzberg, S. L. (2013) TopHat2: accurate alignment of transcriptomes in the presence of insertions, deletions and gene fusions. *Genome Biol.* **14,** R36 CrossRef Medline
33. Feng, J., Meyer, C. A., Wang, Q., Liu, J. S., Shirley Liu, X., and Zhang, Y. (2012) GFOLD: a generalized fold change for ranking differentially expressed genes from RNA-seq data. *Bioinformatics* **28,** 2782–2788 CrossRef Medline
34. Robinson, M. D., McCarthy, D. J., and Smyth, G. K. (2010) edgeR: a Bioconductor package for differential expression analysis of digital gene expression data. *Bioinformatics* **26,** 139–140 CrossRef Medline
35. Ritchie, M. E., Phipson, B., Wu, D., Hu, Y., Law, C. W., Shi, W., and Smyth, G. K. (2015) limma powers differential expression analyses for RNA-sequencing and microarray studies. *Nucleic Acids Res.* **43,** e47 CrossRef Medline
36. Chen, J., Bardes, E. E., Aronow, B. J., and Jegga, A. G. (2009) ToppGene Suite for gene list enrichment analysis and candidate gene prioritization. *Nucleic Acids Res.* **37,** W305–311 CrossRef Medline
37. Fabregat, A., Jupe, S., Matthews, L., Sidiropoulos, K., Gillespie, M., Garapati, P., Haw, R., Jassal, B., Korninger, F., May, B., Milacic, M., Roca, C. D., Rothfels, K., Sevilla, C., Shamovsky, V., *et al.* (2018) The reactome pathway knowledgebase. *Nucleic Acids Res.* **46,** D649–D655 CrossRef Medline
38. Kanehisa, M., Furumichi, M., Tanabe, M., Sato, Y., and Morishima, K. (2017) KEGG: new perspectives on genomes, pathways, diseases and drugs. *Nucleic Acids Res.* **45,** D353–D361 CrossRef Medline
39. Subramanian, A., Tamayo, P., Mootha, V. K., Mukherjee, S., Ebert, B. L., Gillette, M. A., Paulovich, A., Pomeroy, S. L., Golub, T. R., Lander, E. S., and Mesirov, J. P. (2005) Gene set enrichment analysis: a knowledge-based approach for interpreting genome-wide expression profiles. *Proc. Natl. Acad. Sci. U.S.A.* **102,** 15545–15550 CrossRef Medline